DNA Structures

DOI: 10.1002/ange.200602754

A Virus Spotlighted by an Autonomous DNA Machine**

*Yossi Weizmann, Moritz K. Beissenhirtz, Zoya Cheglakov, Roni Nowarski, Moshe Kotler, and Itamar Willner**

We report on an autonomous DNA-based machine that amplifies the detection of M13 phage single-stranded (ss) DNA. The machine is unique in that it makes use of both the genetic and catalytic properties of DNA. Upon recognition of the input viral DNA, the machine is activated and synthesizes a peroxidase-mimicking DNAzyme, which, in turn, generates colorimetric or chemiluminescence readout signals. Multiple rounds of isothermal strand replication, which lead to strand displacement and activation of the DNAzyme moiety, constitute two consecutive levels of signal amplification for this novel detection paradigm that rivals PCR for sensitivity.

Amplification is a fundamental element in bioanalysis. Enzymes,[1] DNAzymes,[2] and lately, nanoparticles[3] or nanocontainers[4] are widely employed for the sensitive detection of biorecognition events. Within these efforts, the amplified and sensitive detection of DNA is particularly challenging and directed to the analysis of pathogens, the detection of genetic disorders, and for forensic applications.[5] PCR provides a general protocol for the amplified detection of DNA. Although the PCR method is time consuming and not free of limitations, it provides the most versatile method to detect minute amounts of DNA. The design of alternative approaches for the sensitive detection of DNA is in continuous demand. Substantial research efforts have been directed lately to the development of DNA-based machines.[6] A DNA-based machine that cleaves RNA by a DNAzyme,[7] DNA-based tweezers,[8,9] autonomous DNA walkers on prearchitectured tracks,[10–13] and signal-triggered switchable structural transformations between duplex DNA and G-quadruplex configurations[14] were reported. The use of the DNA machines as computing systems[15–17] or as sensor systems[18,19] was discussed. Herein we report on an isothermic autonomous DNA machine for the generation of DNAzyme labels. We demonstrate activation of the DNA machine by the analyzed DNA, which allows it to self-detect. The resulting synthesized DNAzyme acts as a peroxidase-mimicking enzyme and as an amplifying label for the analysis of the target DNA. The machine employs colorimetric or chemiluminescent readout signals for the detection of the target DNA. The paradigm developed in the present study represents an approach that might complement or substitute the PCR method. In contrast with the PCR and real-time-PCR (RT-PCR) methods that require thermal replication cycles, costly optical labels, and dedicated instrumentation, the procedure developed by us proceeds isothermally, reaches a sensitivity limit of 10^{-14} M, is cost-effective, and can be visually imaged. The uniqueness of the new paradigm is the amplification of the analyzed DNA by two consecutive steps: the autonomous synthesis and displacement of a nucleic acid that is generated by a biomolecular machine on a DNA template, and the self assembly of the displaced strand into a biocatalytic DNAzyme label that enables the colorimetric or chemiluminescent imaging of the reaction.

The specific DNAzyme synthesized in the present study is a G-quadruplex nucleic acid structure, which intercalates hemin and mimics peroxidase activity.[20,21] In a series of recent studies, we have reported that the hemin/G-quadruplex complex catalyzes the generation of chemiluminescence, in the presence of luminol/H_2O_2, and that it biocatalyzes the oxidation of 2,2′-azino-bis(3-ethylbenzothiazoline-6-sulfonic acid) ($ABTS^{2-}$) by H_2O_2. These biocatalytic reactions were used to develop different DNA-detection assays.[22]

The autonomous synthesis of the DNAzyme is depicted in Figure 1. The template **1**, consisting of three regions, is used as the "track" on which the autonomous synthesis of the DNAzyme is activated. Region I (orange) is complementary to the primer. The segment II (red) is complementary to a nucleic acid that, upon hybridization, yields a double strand that binds the N.BbvC IA nicking endonuclease. Segment III (green) is complementary to the DNAzyme that is synthesized by the machine. Upon the hybridization of the primer **2**, and in the presence of exonuclease-free Klenow (Klenow fragment, exo-) polymerase and the nucleotide mixture (deoxynucleotide triphosphate (dNTPs) act as fuel), the machine is activated. The polymerase-induced reaction replicates the template. Replication of the template, however, yields the double-stranded domain that associates N.BbvC IA and results in the nicking (scission) of the replicated single strand at the marked position. The cleavage of the single strand generates a new site for the initiation of replication. Thus, the polymerase completes the replication of the DNAzyme, and the reactivated replication at the scission site displaces the already synthesized DNAzyme. Subsequently, in the presence of hemin, the autonomous synthesis of the G-quadruplex DNAzyme structure is activated. The DNAzyme catalyzes the oxidation of $ABTS^{2-}$ by H_2O_2 or stimulates the generation of chemiluminescence in the presence of luminol/H_2O_2.

Figure 2 A shows the rate of $ABTS^{2-}$ oxidation by H_2O_2 in the presence of the DNAzymes, which were generated within 5 min by using different concentrations of the template DNA **1**. As the concentration of the template increases, the formation of oxidized $ABTS^{2-}$ is enhanced, implying an

[*] Y. Weizmann, Dr. M. K. Beissenhirtz, Z. Cheglakov, Prof. I. Willner
Institute of Chemistry
The Farkas Center for Light-Induced Processes
The Hebrew University of Jerusalem
Jerusalem 91904 (Israel)
Fax: (+972) 2-6527-715
E-mail: willnea@vms.huji.ac.il
R. Nowarski, Prof. M. Kotler
Department of Experimental Pathology
The Hebrew University–Hadassah Medical School
Jerusalem 91120 (Israel)

[**] This research is supported by the Israel Ministry of Science and by the Minerva Foundation (Moritz K. Beissenhirtz).

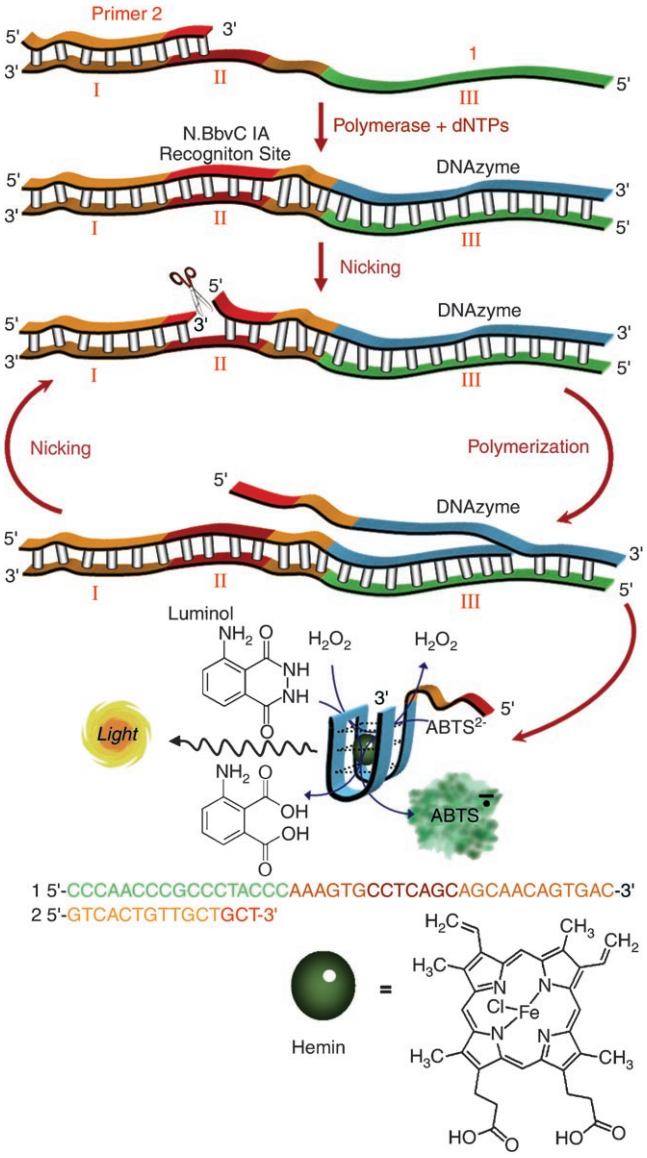

Figure 1. Primer-induced autonomous synthesis of DNAzyme units on template DNA by using polymerase/dNTPs and a nicking enzyme as the biocatalyst.

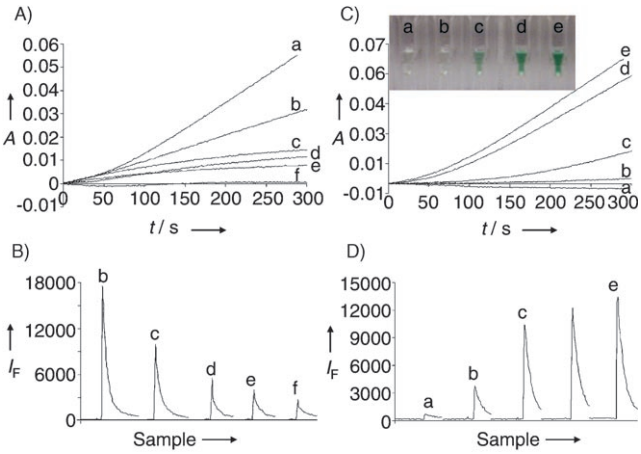

Figure 2. A) Absorbance changes and B) chemiluminescence intensities observed upon the oxidation of $ABTS^{2-}$ by H_2O_2, or the light emission by luminol/H_2O_2 by the DNA-based machine as depicted in Figure 1. Different concentrations of the template **1** were used: a) 1×10^{-6} M, b) 1×10^{-8} M, c) 1×10^{-10} M, d) 1×10^{-12} M, e) 1×10^{-14} M, and f) analysis of the foreign calf-thymus ssDNA (1×10^{-8} M). C) Absorbance changes and D) chemiluminesence intensities observed upon the oxidation of $ABTS^{2-}$ by H_2O_2 or light emission by luminol/H_2O_2 and the DNAzyme synthesized by the DNA-based machine at different time intervals and at the fixed concentrations of **1** (1×10^{-6} M) and **2** (1×10^{-6} M): a) 0 min, b) 10 min, c) 30 min, d) 60 min, e) 90 min. For the absorbance studies, the system included $ABTS^{2-}$ (1.8×10^{-4} M), H_2O_2 (4.4×10^{-5} M), and hemin (4×10^{-7} M). For the chemiluminescence studies, the system included luminol (1×10^{-9} M), H_2O_2 (3×10^{-2} M), and hemin (5×10^{-4} M). Each of the systems were analyzed in a separate vial with a total volume of 50 μL consisting of a buffer solution (NaCl (50 mM), Tris-HCl (10 mM), $MgCl_2$ (10 mM), and dithiothreitol (1 mM); pH 7.9), polymerase (0.4 units), dNTPs (0.2 mM), and N.BbvC IA (0.5 units). The reactions in the respective vials were performed at 37 °C for the specified time intervals and blocked by cooling to 4 °C. The respective colorimetric or chemiluminescence developing solutions consisting of HEPES buffer solution (25 mM), pH 7.4 for the $ABTS^{2-}/H_2O_2$ color test, and pH 9.0 for the luminol/H_2O_2 chemiluminescence assay. KCl (20 mM), NaCl (200 mM), and the respective $ABTS^{2-}/H_2O_2$ or luminol/H_2O_2 substrates were added to the vials to yield a total volume of 200 μL. Absorbance spectra were recorded at $\lambda = 415$ nm. Chemiluminescence was monitored at $\lambda_{em} = 420$ nm. The inset of Figure 2C shows the visual time-dependent color changes upon the oxidation of $ABTS^{2-}$ by the DNAzyme synthesized by the machine. Detailed description of the experimental conditions are provided in the Experimental Section. I_F = fluorescence intensity.

increased content of the generated DNAzyme. Control experiments indicate that oxidation of $ABTS^{2-}$ by H_2O_2 does not occur in the absence of hemin or in the presence of hemin without the generation of the nucleic acid sequence that generates the DNAzyme. Furthermore, exclusion of either the nicking endonuclease, the polymerase, or the dNTPs mixture prohibits the biocatalytic oxidation of $ABTS^{2-}$. Thus, the cooperative polymerization by polymerase, and scission by the nicking enzyme, is essential to self-assemble the DNAzyme in the presence of hemin. The operation of the biomolecular machine was determined by chemiluminescence signals (see Figure 1). The DNAzyme catalyzes the generation of chemiluminescence in the presence of luminol/H_2O_2. Figure 2B shows the chemiluminescence intensities generated by the DNAzymes formed by the biomolecular machine after a time interval of 90 min, in the presence of variable concentrations of the template **1**. The chemiluminescence intensities are enhanced as the concentration of the template is increased, indicating that the contents of the synthesized DNAzymes increase with the template concentration. As before, the different control experiments indicate that all of the components included in the system are essential to drive the synthesis and self-assembly of the DNAzymes. Figure 2C shows the rate of oxidation of $ABTS^{2-}$ by H_2O_2 in the presence of DNAzyme units generated by the biomolecular machine, with a constant concentration of the template **1** (1×10^{-6} M), and at different time intervals. The rate of $ABTS^{2-}$ oxidation is enhanced as the time interval for the formation of the DNAzymes is prolonged. Figure 2D shows the light intensities generated by

DNAzymes formed in the presence of a fixed concentration of the template **1** (1×10^{-6} M) and at different time intervals of the machine operation. As the operation of the biomolecular machine is prolonged, the emitted light intensities are higher, indicating increased contents of the DNAzyme.

The autonomous synthesis of the DNAzyme units, through the operation of the DNA machine, is further confirmed by electrophoretic experiments. Figure 3 depicts

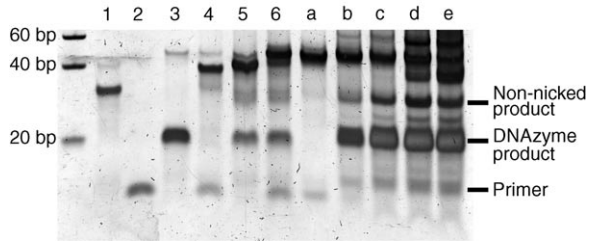

Figure 3. Nondenaturating PAGE analysis of the DNAzyme synthesized by the DNA machine according to Figure 1. 1) Template **1** only, 2) primer **2** only, 3) product (5′-TGAGGCACTTTGGGTAGGG CGGGTTGGG-3′) only, 4) template **1** + primer **2**, 5) template **1** + product, 6) template **1** + primer **2** + product. a)–e) Products generated by the DNA machine at different time intervals, a) $t=0$, b) $t=10$, c) $t=30$, d) $t=60$, and e) $t=90$ minutes. Experimental conditions for the DNA machine operation are as outlined in Figure 2C and D and the details given in the Experimental Section.

the electrophoresis results upon analyzing the model primer DNA **2**, which correspond to the synthesis of the DNAzymes by the DNA machine. Runs a) to e) show the resulting nucleic acid bands generated at different time intervals by the machine. As the operation of the machine is prolonged, the content of the DNAzyme product increases as expected (note that at $t=0$ min no DNAzyme is present). Furthermore, a new band that corresponds in size to the original template is intensified as the operation of the DNA machine is prolonged. This band is attributed to the non-nicked nucleic acid product that is dissociated from the double strand by a thermal treatment prior to electrophoresis (the heat treatment deactivates the enzymes and allows the imaging of the system at a defined time interval). Note that the formation of the double strand between the non-nicked product and the template is inhibited by the competitive association of the excess of DNAzyme to the template. The application of the DNA machine for the amplified analysis of real DNA samples requires the use of an intermediate nucleic acid hairpin structure that is opened by the analyte DNA. The opened stem activates the machine, as depicted in Figure 4. This is exemplified with the analysis of M13 phage ssDNA by using a hairpin probe, and the resulting hybrid triggers the autonomous synthesis of the DNAzyme units. The hairpin structure **3** includes, in the single-stranded loop, the recognition sequence for hybridization with the M13 phage DNA analyte **4**, and upon hybridization with **4**, **3** is opened. The template of the machine **5** includes the domain I, which is complementary to the single-strand nucleic acid of the stem of **3**, and is released upon hybridization with M13 phage DNA. The region II, upon formation of the respective duplex, yields the nicking

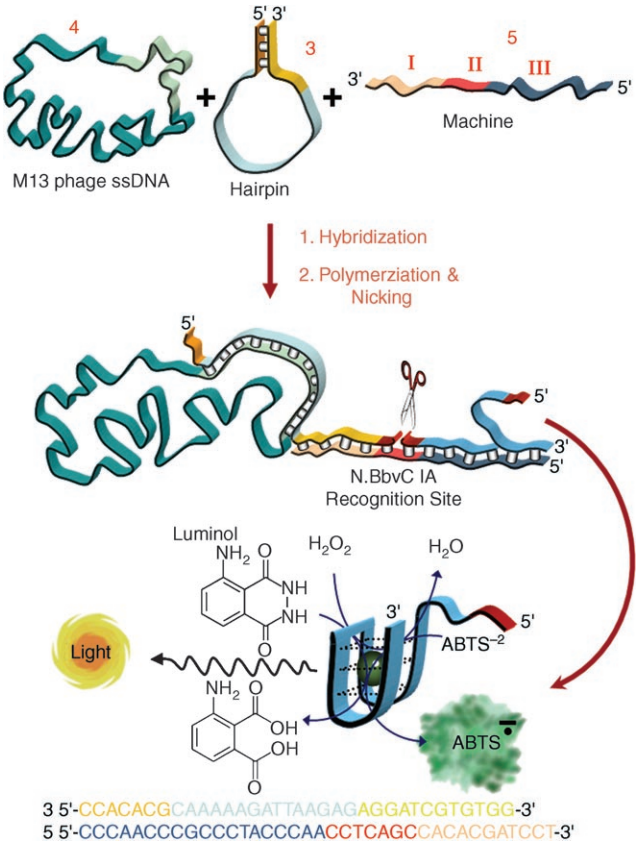

Figure 4. Analysis of M13 phage ssDNA by the hairpin **3** and the DNA-based machine by using template **5**.

site for N.BbvC IA, and the region III is complementary to the DNAzyme sequence. The hybridization of M13 phage DNA with **3** results in the binding of the open hairpin structure to the template **5**. This activates, in the presence of the nucleotide mixture, dNTPs, the polymerase, and the nicking enzyme N.BbvC IA, the autonomous operation of the machine and the synthesis of the DNAzyme. Figure 5 A shows the rate of $ABTS^{2-}$ oxidation by the hemin-functionalized DNAzyme synthesized by the template **5**, upon analyzing different concentrations of M13 phage DNA. The control experiment, in which calf thymus DNA (1×10^{-8} M) is examined by the DNA template, does not lead to any DNAzyme formation and yields a trace oxidation of $ABTS^{2-}$ (Figure 5 A, curve e). Also, in the absence of the M13 phage DNA, or upon exclusion of the hairpin **3**, no oxidation of $ABTS^{2-}$ occurs. A further control experiment revealed that the DNA machine was not triggered by the hairpin **3** in the absence of M13 phage ssDNA. The seven-base stem structure prevents the thermal opening of the hairpin and the non-specific activation of the machine. As the concentration of the analyte decreases, the rate of $ABTS^{2-}$ oxidation decreases, implying that less DNAzyme is synthesized by the machine. The control experiments reveal that the analysis of M13 phage DNA is specific and that the analyte can be detected with a sensitivity limit of 1×10^{-14} M with a signal-to-noise ratio of 2.8. Furthermore, the two readout methods reveal comparable sensitivities. Although the colorimetric assay

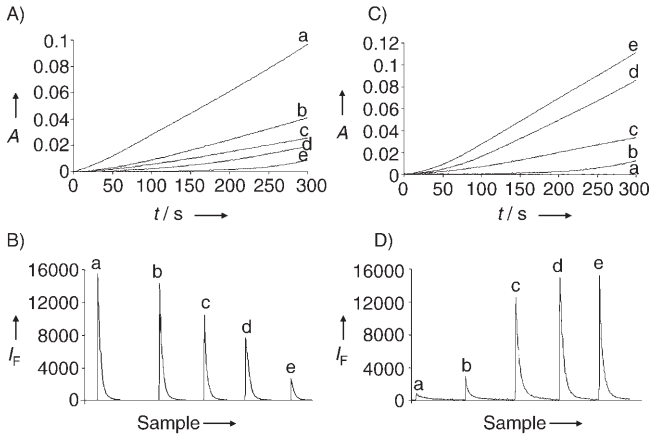

Figure 5. A) Absorbance changes and B) chemiluminescence intensities upon the oxidation of $ABTS^{2-}$ by H_2O_2 or the light emission by luminol/H_2O_2 by the DNA-based machine depicted in Figure 4. Different concentrations of M13 phage ssDNA **4** were analyzed: a) 1×10^{-9} M, b) 1×10^{-11} M, c) 1×10^{-12} M, d) 1×10^{-14} M, and e) analysis of the foreign calf-thymus ssDNA, 1×10^{-8} M. In all systems, fixed concentrations of the hairpin **3** (1×10^{-6} M) and the template **5** (1×10^{-6} M) were employed. Polymerase (0.4 units), dNTPs (0.2 mM), and N.BbvC IA (0.5 units) were included in all of the systems. C) Absorbance changes and D) chemiluminesence intensities upon analyzing M13 phage ssDNA (1×10^{-9} M) by the DNA-based machine at different time intervals and fixed concentrations of **3** (1×10^{-6} M) and **5** (1×10^{-6} M): a) 0 min, b) 10 min, c) 30 min, d) 60 min, and e) 90 min. For the absorbance studies, $ABTS^{2-}$ (1.8×10^{-4} M), H_2O_2 (4.4×10^{-5} M), and hemin (4×10^{-7} M) were included in the system. For the chemiluminescence studies, luminol (1×10^{-9} M), H_2O_2 (3×10^{-2} M), and hemin (5×10^{-4} M) were included in the system. The different measurements were performed in separate vials according to the details provided in the caption of Figure 2. Absorbance spectra were recorded at $\lambda = 415$ nm. Chemiluminescence was monitored at $\lambda_{em} = 420$ nm. Detailed description of the experimental conditions is provided in the Experimental Section.

yields more pronounced signals, the time interval needed to generate the colour response (approximately 250 sec) is an accompanying disadvantage. The chemiluminescence signal is instantaneous, but its translation to a quantitative assay of the analyzed DNA is less accurate. The analysis of the M13 phage ssDNA was also determined by the DNAzyme-generated chemiluminescence, Figure 5B. The generated chemiluminescence decreases in its intensity as the concentration of M13 phage DNA is lowered, and foreign DNA leads to a trace chemiluminescence. Figure 5C shows the rate of $ABTS^{2-}$ oxidation by the DNAzyme and upon analyzing a fixed M13 phage DNA concentration of 1×10^{-9} M. As the time interval for operating the machine is prolonged, the rate of $ABTS^{2-}$ oxidation is enhanced, indicating that the content of synthesized DNAzyme increases with the operating time of the machine. Also, upon analyzing a fixed concentration of M13 phage DNA, the chemiluminescence is intensified as the operation time of the DNA machine is prolonged (see Figure 5D).

In conclusion, the present study has introduced a new paradigm for the sensitive analysis of DNA by using a DNA-based machine that consists of a DNA template, polymerization/nicking enzymes, and strand displacement of the synthesized DNAzyme. The strand displacement and the formation of the DNAzyme represent two consecutive amplification steps in the analytical procedure. Furthermore, we demonstrate that the operation of the DNA machine is triggered by the opening of a predesigned hairpin nucleic acid by the analyte DNA. We also show that the colorimetric or chemiluminescence signals allow the readout of the DNA machine function and operation. The isothermal and rapid (approximately 90 min) analysis of the target DNA, together with the quantitative detection of the analyte, demonstrate the appealing bioanalytical features of the method. This study has substantially broader perspectives for the future development of DNA-based machines, for example, the displaced DNA may be used as a promoter for the aggregation of Au nanoparticles, thus enabling the optical imaging of the analyte through the operation of the machine. Alternatively, the parallel use of several DNA machines may lead to the displacement of nucleic acid barcodes that are analyzed on an array of electrodes (e.g. by electrochemical impedance spectroscopy).

Experimental Section

Materials: Oligonucleotides **1**, **2**, **3**, **5**, the product (5′-TGAGGCACTTTGGGTAGGGCGGGTTGGG-3′; Genosys, Sigma), the deoxynucleotide solution mixture (dNTPs) in NEB buffer solution (NaCl (50 mM), (hydroxymethyl)aminomethane hydrochloride (Tris-HCl; 10 mM), $MgCl_2$ (10 mM), dithiothreitol (1 mM); pH 7.9), the N.BbvC IA endonuclease (New England BioLabs, Inc.), M13 mp18(+) strand DNA, and polymerase Klenow fragment exo- (Amersham Biosciences Corp), and hemin (Frontier Scientific, Inc.) were used without any further purification. A hemin stock solution was prepared in dimethyl sulfoxide (DMSO) and stored in the dark at −20 °C. The single-stranded calf-thymus DNA, luminol, and H_2O_2 were purchased from Sigma.

Colorimetric measurements assay: The experiment was performed in a solution consisting of the products; hemin (4×10^{-7} M), H_2O_2 (4.4×10^{-5} M), and $ABTS^{2-}$ (1.82×10^{-4} M) all in a buffer solution consisting of 2-[4-(2-hydroxyethyl)-1-piperazininyl]ethanesulfonic acid) (HEPES; 25 mM), KCl (20 mM), and NaCl (200 mM); pH 7.4 and at 25 °C. Absorbance changes at 415 nm were followed to characterize the rate of oxidation of $ABTS^{2-}$.

Chemiluminescence measurements: Light-emission experiments were performed by using a photon-counting spectrometer (Edinburgh Instruments, FLS 920) equipped with a cooled photomultiplier detection system, which was connected to a computer (F900 v.6.3 software). Measurements were made in a cuvette that included a buffer solution consisting of HEPES (25 mM), KCl (20 mM), and NaCl (200 mM); pH 9.0 and hemin (1×10^{-9} M), luminol (0.5 mM), and H_2O_2 (30 mM). The light emission was monitored at $\lambda_{em} = 420$ nm.

Received: July 11, 2006
Revised: August 22, 2006
Published online: October 11, 2006

Keywords: biosensors · chemiluminescence · DNA structures · DNAzymes · enzymes

[1] D. J. Caruana, A. Heller, *J. Am. Chem. Soc.* **1999**, *121*, 769–774.
[2] Y. Xiao, V. Pavlov, T. Niazov, A. Dishon, M. Kotler, I. Willner, *J. Am. Chem. Soc.* **2004**, *126*, 7430–7431.

[3] J. Wang, G. Liu, A. Merkoçi, *J. Am. Chem. Soc.* **2003**, *125*, 3214 – 3215.
[4] J. Wang, O. Rincon, R. Polsky, E. Dominguez, *Electrochem. Commun.* **2003**, *5*, 83 – 86
[5] J. J. Gooding, *Electroanalysis* **2002**, *14*, 1149 – 1156.
[6] a) F. C. Simmel, W. U. Dittmer, *Small* **2005**, *1*, 284 – 299; b) M. K. Beissenhirtz, I. Willner, *Org. Biolmol. Chem.* **2006**, *4*, 3392 – 3401.
[7] J. Liu, Y. Lu, *J. Am. Chem. Soc.* **2003**, *125*, 6642 – 6643.
[8] B. Yurke, A. J. Turberfield, A. P. Mills Jr., F. C. Simmel, J. L. Neumann, *Nature* **2000**, *406*, 605 – 608.
[9] Y. Chen, M. Wang, C. Mao, *Angew. Chem.* **2004**, *116*, 3638 – 3641; *Angew. Chem. Int. Ed.* **2004**, *43*, 3554 – 3557.
[10] J.-S. Shin, N. A. Pierce, *J. Am. Chem. Soc.* **2004**, *126*, 10834 – 10835.
[11] W. B. Sherman, N. C. Seeman, *Nano Lett.* **2004**, *4*, 1203 – 1207.
[12] P. Yin, H. Yan, X. G. Daniell, A. J. Turberfield, J. H. Reif, *Angew. Chem.* **2004**, *116*, 5014 – 5019; *Angew. Chem. Int. Ed.* **2004**, *43*, 4906 – 4911.
[13] J. Bath, S. J. Green, A. J. Turberfield, *Angew. Chem.* **2005**, *117*, 4432 – 4435; *Angew. Chem. Int. Ed.* **2005**, *44*, 4358 – 4361.
[14] P. Alberti, J.-L. Mergny, *Proc. Natl. Acad. Sci. USA* **2003**, *100*, 1569 – 1573.
[15] Y. Benenson, B. Gil, U. Ben-Dor, R. Adar, E. Shapiro, *Nature* **2004**, *429*, 423 – 429.
[16] Y. Benenson, R. Adar, T. Paz-Elizur, Z. Livneh, E. Shapiro, *Proc. Natl. Acad. Sci. USA* **2003**, *100*, 2191 – 2196.
[17] M. N. Stojanovic, D. Stefanovic, *Nat. Biotechnol.* **2003**, *21*, 1069 – 1074.
[18] Y. Weizmann, Z. Cheglakov, V. Pavlov, I. Willner, *Angew. Chem.* **2006**, *118*, 2296 – 2300; *Angew. Chem. Int. Ed.* **2006**, *45*, 2238 – 2242.
[19] S. Beyer, F. C. Simmel, *Nucleic Acids Res.* **2006**, *34*, 1581 – 1587.
[20] P. Travascio, P. K. Witting, A. G. Mauk, D. Sen, *J. Am. Chem. Soc.* **2001**, *123*, 1337 – 1348.
[21] P. Travascio, Y. Li, D. Sen, *Chem. Biol.* **1998**, *5*, 505 – 517.
[22] a) T. Niazov, V. Pavlov, Y. Xiao, R. Gill, I. Willner, *Nano Lett.* **2004**, *4*, 1683 – 1687; b) z. Cheglakov, Y. Weizmann, M. K. Beissenhirz, I. Willner, *Chem. Comm.* **2006**, 3205 – 3207.

